Organometallics **2001,** *20,* 3543−3549

Redox Potential Selection in a New Class of Dendrimers Containing Multiple Ferrocene Centers

Julio Alvarez, Tong Ren, and Angel E. Kaifer*

Center for Supramolecular Science and Department of Chemistry, University of Miami,
Coral Gables, Florida 33124-0431

Received March 6, 2001

The preparation and electrochemical properties of four new dendrimers, compounds **1**, **2**, **3**, and **4**, containing eight, seven, four, and four ferrocene residues, respectively, are described. These small dendrimers were prepared with the building block bis(ferrocenylmethyl)-alkylamine, which contains the tether $-CH_2-N(R)-CH_2-$ linking two ferrocene units. The resulting dendrimers are multiferrocene compounds in which the peripheral ferrocene residues are paired. Partial protonation or *N*-methylation of the connecting nitrogen atoms allows the selection of the ferrocene oxidation potentials between two different values (~0.4 and ~0.6 V vs Ag/AgCl). The observed voltammetric pattern for ferrocene oxidation can be reversibly switched among several states depending on the number of protonated centers within each dendritic structure. Crystallographic and electrochemical data confirm that the electronic communication between two equivalent ferrocene centers is lessened after protonation or *N*-methylation of the connecting nitrogens.

Introduction

Macromolecular systems containing several metallocene centers with varying degrees of interaction have attracted considerable attention.[1] Independently, some of the extensive research work on metallodendrimers[2] has explored the functionalization with metallocene residues of the periphery of these macromolecular structures.[3] The appeal of such systems relies on the spatial proximity of the metal centers that may result in electronic communication throughout the dendritic structure. This may lead to new materials with substantial electron mobility and interesting electrical and redox properties.[2] Electrochemical studies with dendrimers containing multiple metallic centers usually have to contend with problems related to the adsorption of electrogenerated species on the electrode surface. These problems are due to the considerable changes in polarity and electrical charge associated with the electron transfer reactions, which make it almost impossible to find a single solvent system to efficiently dissolve the two extreme redox states, that is, the state with all centers reduced and the state with all centers oxidized. Usually, dendrimers containing multiple redox centers on their peripheries undergo electron transfer reactions around a single potential value, reflecting poor electronic communication among the redox centers.[3] An important exception to this trend has been reported by the group of Morán and Cuadrado, who successfully achieved the preparation of a silicon-based, ferrocene dendrimer with unambiguous electronic communication among the peripheral ferrocene units in the dendritic structure.[4]

In previous work[5] we have prepared and characterized a new series of dinuclear ferrocene compounds connected by the bridge $-CH_2-N(R)-CH_2-$. An interesting feature of these compounds is that the extent of electronic communication between the ferrocene centers can be controlled in several ways. For example, by changing the steric bulk of the group R, attached to the nitrogen atom in the middle of the bridge, we have observed comproportionation constant values (K_c) varying from 220 to 34.[5b] *N*-Methylation or protonation of the bridging nitrogen also diminished the extent of electronic communication (Scheme 1), lowering the comproportionation constants to values close to the statistical minimum of 4 expected when the degree of

---

* Corresponding author. Tel: (305) 284-3468. Fax: (305) 444-1777. E-mail: akaifer@miami.edu.

[1] (a) Barlow, S.; O'Hare, D. *Chem. Rev.* **1997**, *97*, 637. (b) Nguyen, P.; Gómez-Elipe, P.; Manners, I. *Chem. Rev.* **1999**, *99*, 1515.

[2] For an excellent review on metallodendrimers, see: Newkome, G. R.; He, E.; Moorefield, C. N. *Chem. Rev.* **1999**, *99*, 1689.

[3] (a) Moulines, F.; Djakovitch, L.; Boese, R.; Gloaguen, B.; Theil, W.; Fillaut, J.-L.; Delville, M.-H.; Astruc, D. *Angew. Chem., Int. Ed. Engl.* **1993**, *32*, 1075. (b) Alonso, B.; Cuadrado, I.; Morán, M.; Losada, J. *J. Chem. Soc., Chem. Commun.* **1994**, 2575. (c) Fillaut, J.-L.; Linares, J.; Astruc, D. *Angew. Chem., Int. Ed. Engl.* **1994**, *33*, 2460. (d) Cuadrado, I.; Morán, M.; Casado, C. M.; Alonso, B.; Lobete, F.; García, B.; Ibisate, M.; Losada, J. *Organometallics* **1996**, *15*, 5278. (e) Valerio, C.; Fillaut, J.-L.; Ruiz, J.; Guittard, J.; Blais, J.-C.; Astruc, D. *J. Am. Chem. Soc.* **1997**, *119*, 2588. (f) Castro, R.; Cuadrado, I.; Alonso, B.; Casado, C. M.; Morán, M.; Kaifer, A. E. *J. Am. Chem. Soc.* **1997**, *119*, 5760. (g) Takada, K.; Díaz, D. J.; Abruña, H. D.; Cuadrado, I.; Casado, C. M.; Alonso, B.; Morán, M.; Losada, J. *J. Am. Chem. Soc.* **1997**, *119*, 10763. Shu, C.-F.; Shen, H.-M. *J. Mater. Chem.* **1997**, *7*, 47. (h) Deschenaux, R.; Serrano, E.; Levelut, A. M. *Chem Commun.* **1997**, 1577. (i) González, B.; Casado, C. M.; Alonso, B.; Cuadrado, I.; Morán, M.; Wang, Y.; Kaifer, A. E. *Chem. Commun.* **1998**, 2569. (j) Kayser, B.; Altman, J.; Nöth, H.; Knizek, J.; Beck, W. *Eur. J. Inorg. Chem.* **1998**, *1*, 1791. (k) Valerio, C.; Alonso, E.; Ruiz, J.; Blais, J.-C.; Astruc, D. *Angew. Chem., Int. Ed. Engl.* **1999**, *38*, 1747. (l) Nlate, S.; Ruiz, J.; Blais, J.-C.; Astruc, D. *Chem. Commun.* **2000**, 417−418. (m) Casado, C. M.; González, B.; Cuadrado, I.; Alonso, B.; Morán, M.; Losada, J. *Angew. Chem., Int. Ed.* **2000**, *39*, 2139. (n) Nlate, S.; Ruiz, J.; Blais, J.-C.; Astruc, D. *Chem. Eur. J.* **2000**, *6*, 2544.

[4] Cuadrado, I.; Casado, C. M.; Alonso, B.; Morán, M.; Losada, J.; Belsky, V. *J. Am. Chem. Soc.* **1997**, *119*, 7613.

[5] (a) Alvarez, J.; Kaifer, A. E. *Organometallics* **1999**, *18*, 5733. (b) Alvarez, J.; Ni, Y.; Ren, T.; Kaifer, A. E. *J. Supramol. Chem.* **2001**, *1*, in press.

10.1021/om0101792 CCC: $20.00
Publication on Web 07/07/2001

Scheme 1

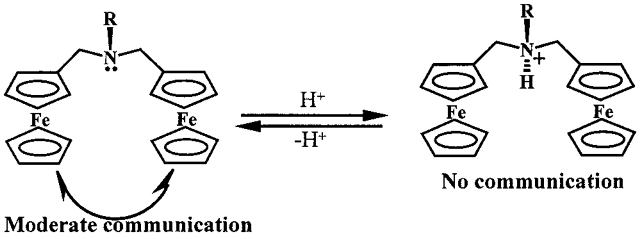

interaction is null.[6] Since an important difference between methylation and protonation is that the former is irreversible while the latter is not, we were able to regulate reversibly the extent of electronic interaction between the ferrocene units just by adding acid and base. In all the cases, the crystallographic evidence indicated that these effects were associated with concomitant changes in the distance and orientation between the ferrocene centers.[5b] Other factors, such as the variable polarizability of the bridge, may also affect the level of inter-ferrocene communication.[7]In this paper, we report the preparation and electrochemistry of a series of four new compounds based on this formerly investigated[5] dinuclear ferrocene building block, now expressed in oligomeric structures with dendritic character (see structures). The multiple presence of the dinuclear ferrocene motifs in the surface of these compounds may introduce a degree of steric crowding that could elicit significant intramolecular electronic communication within the dendrimer. At the same time, we hoped to retain a measure of control on the levels of electronic communication through the bridging fragments $-CH_2-NR-CH_2-$, as in the case of the dinuclear ferrocene compounds.[5] On the other hand, *N*-methylation or protonation of the nitrogen bridges gives rise to a significant positive shift (0.1 to 0.2 V) in the formal potential for the oxidation of the ferrocene units. Therefore, partial protonation of oligomers **1**−**3** should lead to molecular species in which the relative number of ferrocene units undergoing oxidation at two different potentials (corresponding to the protonated and unprotonated branches) can be determined by the extent of protonation, i.e., by gradual additions of acid or base.

Experimental Section

Materials. All solvents and chemicals for synthesis were commercially available or reagent grade quality and were used without any further purification. Solvents were removed on a rotary evaporator connected to a water-aspirator vacuum, and the remaining traces were evaporated in a vacuum oven typically set at 70 °C overnight. For electrochemistry, acetonitrile and dichloromethane (99.9%, HPLC grade) were purchased from Sigma-Aldrich.

Methods and Instrumentation. ^{1}H NMR spectra were recorded on a Varian VXR-400 spectrometer, and chemical shifts were measured with reference to the residual solvent signals. Mass spectra (FAB, nitrobenzyl alcohol matrix) were recorded on a VG Trio-2 mass spectrometer. Electrochemical measurements were performed with a BAS 100W analyzer equipped with a standard three-electrode cell. For all electrochemical techniques, the reference electrode was Ag/AgCl. Voltammetric experiments were performed using a glassy carbon disk (ca. 0.018 cm^2) as the working electrode and a platinum wire as the auxiliary electrode. The pulse parameters for Osteryoung square wave voltammetry (OSWV) were as follows: square wave frequency, 15 Hz; potential step, 4 mV; square wave amplitude, 25 mV. Under these conditions the effective scan rate was 60 mV/s. The parameters for normal pulse voltammetric experiments (NPV) were as follows: scan rate, 30 mV/s; sample width, 17 ms; pulse width, 50 ms; pulse period, 200 ms.

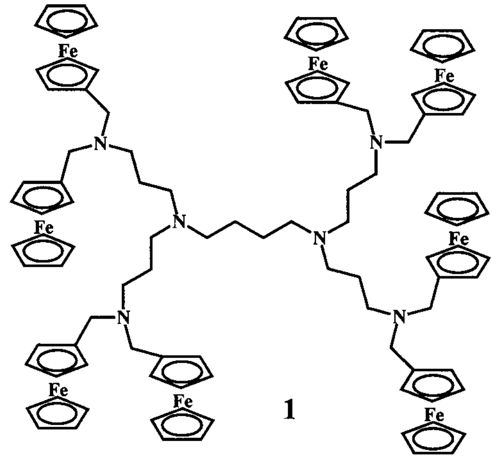

1

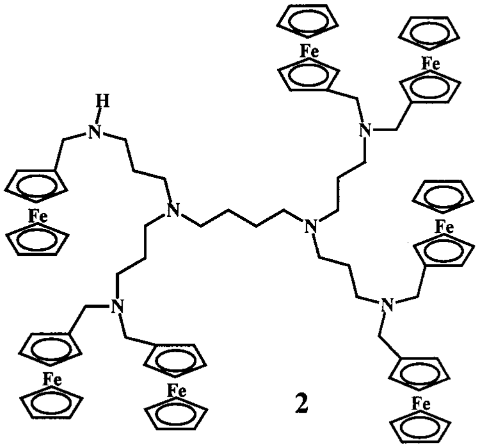

2

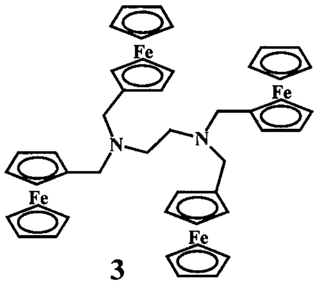

3

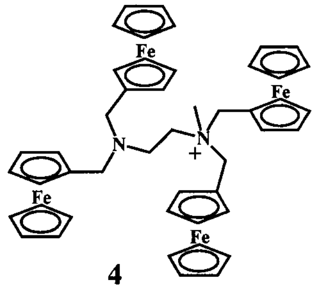

4

Typically, a solution containing 0.2 mM oligomeric ferrocene compound and 0.2 M tetrabutylammonium hexafluorophos-

---

[6] Flanagan, J.; Margel, S.; Bard, A. J.; Anson, F. C. *J. Am. Chem. Soc.* **1978**, *100*, 4248.

[7] Southard, G. E.; Curtis, M. D. *Organometallics* **2001**, *20*, 508.

phate was prepared using an acetonitrile−dichloromethane solvent mixture having a composition chosen to minimize adsorption/precipitation effects. Protonation and deprotonation experiments were performed by microliter additions of aqueous 1 N HCl and 0.5 N NaOH solutions (Fisher) to a 2 mL volume of solution in the electrochemical cell. In some cases, cyclic voltammograms were fitted and simulated using the DigiSim software package,[8] version 2.1. Bulk electrolysis experiments under potentiostatic conditions were performed with platinum mesh electrodes in a two-compartment electrochemical cell.

Synthesis of Tetrakis(di(ferrocenylmethyl))polypropylenimine Tetraamine (1). (Ferrocenylmethyl)trimethylammonium iodide (1.6 g, 4.16 mmol) was dissolved in 10 mL of acetonitrile and reacted with polypropylenimine tetraamine dendrimer (Aldrich) (0.170 mL, 0.52 mmol) in the presence of potassium carbonate (1.4 g, 10 mmol). After reflux for 10 h, a sticky orange precipitate appeared and the reaction was stopped. The precipitate was collected and dissolved in dichloromethane to separate the excess carbonate. Mass spectrometry confirmed the presence of the octasubstituted derivative in the dissolved precipitate, along with other products also evident by thin-layer chromatography. Column chromatography with normal silica gel (4% v/v triethylamine in ethyl acetate−methanol, 80:20) allowed the isolation of a pure compound ($R_f = 0.4$) that was characterized as the octaferrocenyl dendrimer (**1**). The oily orange product was obtained in a 20% yield. ^{1}H NMR ($CDCl_3$): 4.17(t, 16H, C_5H_4), 4.12(t, 16H, C_5H_4), 4.09(s, 40H, C_5H_5), 3.41(s, 16H, CH_2), 2.26(m, 20H, $10CH_2$, overlapped), 1.34(m, 8H, $4CH_2$), 1.25(m, 4H, $2CH_2$). ^{13}C {^{1}H} NMR ($CDCl_3$): (77.20, 70.18, 67.81) C_5H_4, 68.50 C_5H_5, 52.62, 52.27, 50.57, 29.67, 25.06, $6CH_2$ overlapped. MS (FAB, *m/z*): 1900 (M^+). Anal. Calcd for $C_{104}H_{120}N_6Fe_8$: C, 65.71; H, 6.36. Found: C, 65.10; H, 6.28.

Synthesis of Tris(di(ferrocenylmethyl))(ferrocenylmethyl)polypropylenimine Tetraamine (2). From the crude mixture obtained in the previous reaction a second band ($R_f = 0.2$) was isolated by column chromatography in 40% yield. Similar in color and physical appearance to the octaferrocenyl dendrimer, this compound turned out to be the heptasubstituted derivative (**2**). ^{1}H NMR ($CDCl_3$): 4.17 to 4.09-(m, 63H, C_5H_4 and C_5H_5, overlapped), 3.51(s, 2H, CH_2), 3.40-(s, 12H, $6CH_2$), 2.62(t, 2H, CH_2), 2.43 to 2.26(m, 18H, $9CH_2$, overlapped), 1.57(m, 8H, $4CH_2$, overlapped), 1.34(m, 4H, $2CH_2$, overlapped). ^{13}C {^{1}H} NMR ($CDCl_3$): (77.21, 70.16, 68.50, 68.40, 67.78) C_5H_4 and C_5H_5, (54.33, 52.63, 52.30, 52.25, 50.65, 49.20, 48.30, 27.62, 25.09) CH_2, overlapped. MS (FAB, *m/z*): 1700 (M^+). Anal. Calcd for $C_{93}H_{110}N_6Fe_7$: C, 65.60; H, 6.52. Found: C, 65.53; H, 6.48.

Synthesis of Bis(di(ferrocenylmethyl))ethylenediamine (3). Ethylenediamine (Aldrich) (0.067 mL, 1 mmol) was dissolved in 10 mL of acetonitrile and refluxed for 5 h with (ferrocenylmethyl)trimethylammonium iodide (1.65 g, 4 mmol) in the presence of potassium carbonate (1.4 g, 10 mmol). Diethyl ether was added to the crude mixture to precipitate any remaining (ferrocenyl)trimethylammonium salt and potassium carbonate. The precipitate were filtered off and washed with dichloromethane. The filtrate was then evaporated to dryness and redissolved in dichloromethane to allow further precipitation of carbonate. Recrystallization from a chloroform−hexane mixture gave the pure tetraferrocenyl oligomer as large and robust orange needles in 80% yield. ^{1}H NMR ($CDCl_3$): 4.11(s, 16H, C_5H_4, overlapped), 4.063(s, 20H, C_5H_5), 3.35(s, 8H, $4CH_2$), 2.30(s, 4H, $2CH_2$). ^{13}C{^{1}H} NMR ($CDCl_3$): (77.20, 70.28, 67.81) C_5H_4, 68.47 C_5H_5, 53.12 CH_2, 48.69 CH_2. MS (FAB, *m/z*): 853 (MH^+). Anal. Calcd for $C_{46}H_{48}N_2Fe_4$: C, 64.83; H, 5.68. Found: C, 64.65; H, 5.81.

Monomethylation of Compound 3 (4). Tetramer **3** (0.853 g, 1 mmol) and iodomethane (0.062 mL, 1 mmol) were dissolved in 20 mL of acetonitrile. After 2 h of reaction at room temperature the mixture was concentrated and the methylated product was precipitated by addition of ether. Additional precipitation steps produced a yellow powder in 85% yield. Ion exchange to obtain the hexafluorophosphate salt was carried out using NH_4PF_6 in acetonitrile and further precipitation with water. Single crystals for X-ray diffraction analysis and NMR characterization were grown from solutions of the iodide salt in ethyl acetate−hexane. ^{1}H NMR ($CDCl_3$): 4.61(d, 2H, CH_2), 4.43(d, 2H, CH_2), 4.38, 4.33, 4.28(s, 8H, C_5H_4), 4.24(s, 10H, C_5H_5), 4.24(t, 4H, C_5H_4), 4.20(t, 4H, C_5H_4), 3.49(s, 4H, $2CH_2$), 3.30(t, 2H, CH_2), 2.68(t, 2H, CH_2), 2.50(s, 3H, CH_3). ^{13}C{^{1}H} NMR ($CDCl_3$): 77.21, 72.38, 72.34, 72.14, 70.28, 70.22, 69.55, 68.91, 68.52, 62.26, 56.42, 54.61, 45.67, 45.08. MS (FAB, *m/z*): 868 (M^+). Anal. Calcd for $C_{47}H_{51}N_2Fe_4PF_6$: C, 55.73; H, 5.08. Found: C, 55.66; H, 5.16.

X-ray Structure Determinations of Compounds 3 and 4. Single crystals of compounds **3** and **4** were grown by slow evaporation of chloroform−hexane and ethyl acetate−hexane solutions, respectively. Diffraction data were collected at 300 K on a Bruker SMART1000 CCD-based X-ray diffractometer equipped with a Mo-target X-ray tube ($\lambda = 0.71073$ Å). Data were measured using ω scans of 0.3° per frame during 10 s such that a hemisphere was collected. No decay was detected for either one of two data sets collected, as indicated by the re-collection of the first 50 frames at the end of each data acquisition. The frames were integrated with the Bruker SAINT software package using a narrow-frame integration algorithm, which also corrects for Lorentz and polarization effects.[9] Absorption corrections were applied using SADABS supplied by George Sheldrick.[10]

Both structures were solved using the Bruker SHELXTL software package version 5.1.[11−13] Space groups for crystals **3** and **4** were unambiguously assigned as $P\bar{1}$ and $P2_1/c$, respectively. The asymmetric unit of **3** consists of one-half of the tetramer, which is related to the other half via an inversion center. The asymmetric unit of **4** contains one cation−anion pair. The iodide anion in **4** was translationally disordered over two sites separated by 0.349 Å, which were refined with the occupancy constraint to convergence. The structures of **3** and **4** were refined to convergence by the least-squares method on F^2, SHELXL-93, incorporated in SHELXTL.PC V 5.03, with all non-hydrogen atoms being anisotropic and all hydrogen atoms in calculated position and riding mode. The final least-squares refinements converged at the *R*-factors reported in Table 1, along with other procedure parameters. Full tables of atomic coordinates, bond lengths and angles, anisotropic displacements, and torsional angles are provided as Supporting Information (Tables S1−S8).

Results and Discussion

Synthesis. The dendritic compounds **1**−**3** were prepared by reaction of (ferrocenylmethyl)trimethylammonium iodide[14] with the corresponding primary amine following a procedure previously reported by us.[5] This reaction readily converts a primary amine (RNH_2) into a dinuclear ferrocene compound that can be formulated as Fc−CH_2−N(R)−CH_2−Fc (Fc = ferrocene). In this work, we have used either 1,2-diaminoethane or a dendrimer precursor with four branches terminated in

---

[8] Rudolph, M.; Reddy, D. P.; Feldberg, S. W. *Anal. Chem.* **1994**, *66*, 589A.

[9] *Saint V 6.035 Software for the CCD Detector System*; Bruker-AXS Inc., 1999.

[10] Blessing, B. *Acta Crystallogr.* **1995**, *A51*, 33.

[11] Sheldrick, G. M. *SHELXS-90, Program for the Solution of Crystal Structures*; University of Göttigen, Germany, 1990.

[12] Sheldrick, G. M. *SHELXL-93, Program for the Refinement of Crystal Structures*; University of Göttigen, Germany, 1993.

[13] *SHELXTL 5.03 (Windows-NT Version), Program Library for Structure Solution and Molecular Graphics*; Bruker-AXS Inc., 1998.

[14] Lombardo, A.; Bieber, T. I. *J. Chem. Educ.* **1983**, *60*, 1080.

Table 1. Crystal Data and Structure Refinement for Compounds 3 and 4

	3	**4**
empirical formula	$C_{26}H_{48}N_2Fe_4$	$C_{47}H_{51}N_2Fe_4I$
fw	852.26	994.20
space group	$P\bar{1}$	$P2_1/c$
a, Å	7.6010(8)	16.2491(7)
b, Å	10.8409(11)	10.1974(5)
c, Å	13.0416(14)	25.6676(12)
α, deg	65.856(2)	
β, deg	82.467(2)	91.009(1)
γ, deg	88.612(2)	
volume, Å^3	971.66(18)	4252.4(3)
Z	1	4
$D_{\text{calc.}}$, g cm^3	1.456	1.553
cryst size, mm	0.33 × 0.23 × 0.12	0.17 × 0.11 × 0.04
μ, mm^{-1}	1.498	2.098
λ(Mo Kα), Å	0.71073	0.71073
temperature, °C	27(2)	27(2)
no. of reflns collected	5135	22 040
no. of ind reflns	3370 [R(int) = 0.0129]	7483 [R(int) = 0.0367]
final R indices [$I > 2\sigma(I)$][a]	R1 = 0.030, wR2 = 0.072	R1 = 0.033, wR2 = 0.071
R indices (all data)	R1 = 0.039, wR2 = 0.075	R1 = 0.056, wR2 = 0.087

[a] $R1 = \sum||F_o| - |F_c||/\sum|F_o|$, $wR2 = (\sum w(F_o^2 - F_c^2)^2/\sum w(F_o^2)^2)^{1/2}$.

primary amine functionalities. The diamine led to the tetrameric ferrocene **3**, and the tetrameric amine yielded the octameric ferrocene **1**. However, the second reaction also produced an even larger yield of **2**. This compound contains seven peripheral ferrocene residues and can be considered as a "defective" analogue of **1**, in which one of the dinuclear ferrocene motifs is incomplete. We isolated and fully characterized **2** because of our interest in dendrimers having nonequivalent redox centers. Unfortunately, we found that the electrochemical behavior of **2** is very similar to that of **1** (vide infra), suggesting that the unique ferrocene residue in **2** is not significantly different from the other six ferrocene residues.

Reaction of **3** with 1 equiv of iodomethane produced the monomethylated compound **4**. We did not detect the formation of the dimethylated analogue, probably as a reflection of the unfavorable Coulombic repulsion that would exist in this compound due to the proximity of the two positively charged nitrogen atoms. With the only exception of this compound (**4**) the remaining derivatives exhibit very limited solubility in solvents of intermediate polarity, such as methanol and acetonitrile, but good solubility in chloroform and hexane. For this reason voltammetric experiments were performed in nonpolar solvents that cannot effectively dissolve highly charged molecules, giving rise to the observation of adsorption effects with the electrogenerated species.

Electrochemical Results. Due to these adsorption problems, the determination of formal potentials ($E^{\circ\prime}$) was carried out with NPV, a particularly suitable technique for cases in which the electrogenerated species is insoluble in the reaction medium. The collected potential values (before and after full protonation) are given in Table 2. Note that, as mentioned before, these data show no significant formal potential differences between compounds **1** and **2**. However, *coulometric measurements in bulk electrolytic experiments under potential control yielded values of 8 and 7 electrons per molecule*, respectively, in perfect agreement with the structures of both compounds. Therefore, the voltammetric behavior of both dendrimers indicates that their ferrocene centers are noninteracting and essentially equivalent. The structurally distinct (unpaired) ferrocene center in **2** behaves similarly to the remaining ferrocene centers in this small dendrimer. Furthermore, the moderate level of electronic communication between the two ferrocene centers that is observed in dimeric compounds containing the $-CH_2-N(R)-CH_2-$ tether cannot be detected in these dendrimers. This finding probably results from the intrinsically broader nature of the voltammetric wave corresponding to 7 or 8 electron transfers in the dendritic (oligomeric) systems. The intrinsic breadth of the voltammetric wave limits the potential resolution and prevents the observation of the moderate levels of communication that may exist between the paired ferrocene centers in each of the dendrimer branches.

Table 2. Effects of Protonation on the Formal Potential[a] for the Oxidation of Compounds 1−3 in $CH_2Cl_2-CH_3CN$ (80:20, v/v) and 4 in Pure CH_3CN at 25 °C

compound	unprotonated $E^{\circ\prime}$ (V vs Ag/AgCl)	protonated $E^{\circ\prime}$ (V vs Ag/AgCl)
1[b]	0.50	0.61
2[b]	0.51	0.61
3[b]	0.45	0.61
4[c]	0.48 and 0.67	0.62

[a] All solutions contained 0.2 mM **1**−**4** and 0.2 M $BuNPF_6$ as supporting electrolyte. [b] Determined by NPV assuming that $E^{\circ\prime} = E_{1/2}$. [c] Determined by CV assuming that $E^{\circ\prime} = E_{1/2}$.

As we have previously reported[5] the protonation or *N*-methylation of dinuclear ferrocene compounds with a $-CH_2-N(R)-CH_2-$ bridge shifts the average formal potential for the oxidation of the ferrocene centers to more positive values. The magnitude of this shift ranges from 0.1 to 0.2 V, and the potential shift itself is due to the electron-withdrawing effect induced by the positively charged nitrogen atom in the bridge between the ferrocenes. This property opens a very interesting possibility with compounds **1**−**3**, which contain several peripheral basic sites (tertiary nitrogens), each affecting the oxidation potential of two attached ferrocene centers. For instance, Figure 1 shows the voltammetric behavior of **1** in a $CH_3CN-CH_2Cl_2$ mixture (1:4, v/v), in the absence of acid and in the presence of 3.5 and 10 equiv of HCl. Before the addition of acid the voltammogram is dominated by an oxidation wave at an apparent half-wave potential ($E_{1/2}$) of ∼0.5 V (a small adsorption postwave is also visible). Upon addition of 3.5 equiv of HCl, the voltammogram clearly shows two voltammetric waves, which merge into a single wave ($E_{1/2} = \sim 0.6$ V) upon addition of excess HCl (10 equiv). Obviously, the voltammetric wave at ∼0.5 V corresponds to ferrocene units attached to free nitrogen atoms, while the voltammetric wave at ∼0.6 V results from ferrocene residues connected to protonated nitrogen atoms. Titration experiments show that the two-wave behavior exhibited at 3.5 equiv of HCl reflects the partial protonation of **1**. As the degree of protonation increases, the currents associated with the wave at more positive potential increase at the expense of the currents associated with the first wave. Upon addition of excess HCl, protonation of **1** is complete, leading to the observation of a single voltammetric wave. We have not performed quantitative

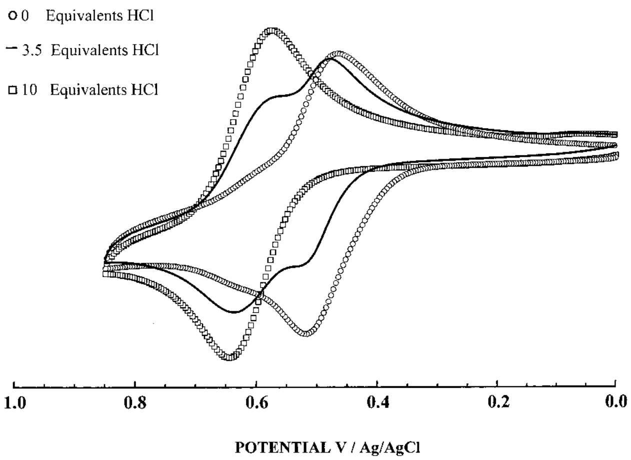

Figure 1. Voltammetric response of dendrimer **1** illustrating three points in an electrochemical titration with aqueous 1 N HCl. The solution was 0.2 mM **1** and 0.2 M Bu_4NPF_6 in CH_2CL_2–CH_3CN (80:20 v/v). Working electrode: glassy carbon (0.018 cm^2). Scan rate: 0.1 V/s.

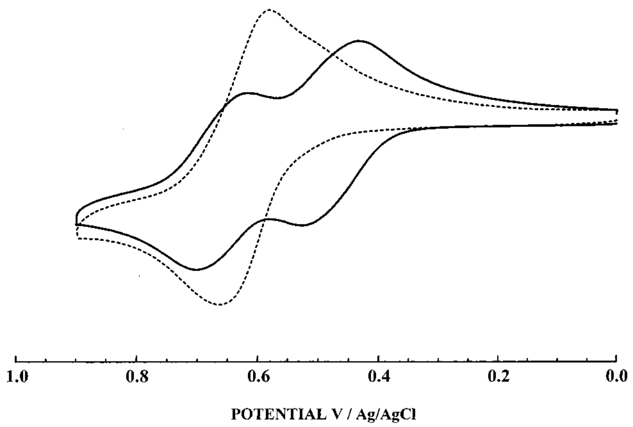

Figure 2. Voltammetric behavior of compound **4** before (continuous line) and after protonation with a 10-fold excess of aqueous HCl (dotted line). The solution was 0.2 mM **4** and 0.2 M Bu_4NPF_6 in CH_3CN. Working electrode: glassy carbon (0.018 cm^2). Scan rate: 0.1 V/s.

Scheme 2

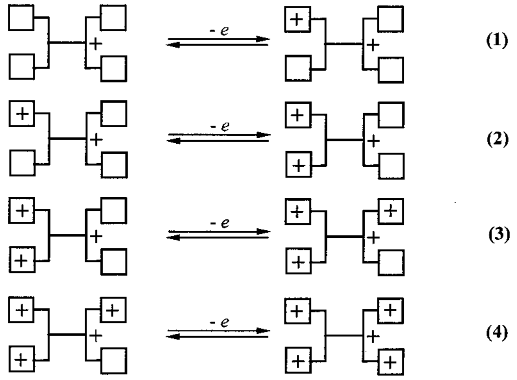

measurements of the pK_a values corresponding to all the basic sites in dendrimers **1**–**4**. However, the observed behavior clearly reveals that it is possible to determine the fraction of ferrocene residues in **1** that will be oxidized at each of the two potentials by adjusting the extent of protonation using simple acid/base reactions. Dendrimer **1** (as well as **2** and **3** to lesser degrees) affords an interesting example of coupling between electron and proton transfer processes. In these dendrimers, the redox potentials for multiple electron transfers can be selected (between two values) by proton transfer reactions. There are certainly other examples[15] of oligomeric ferrocene systems that exhibit two or more resolved oxidation waves. However, in those systems the voltammetric oxidation pattern is fixed, while in the small dendrimers reported here the voltammetric pattern can be changed by proton transfer reactions.

The voltammetric behavior of compound **4** shows two redox waves before any acid additions (Figure 2). This is exactly as expected due to the presence of two dinuclear ferrocene groupings that are different because one of them bears a positive charge due to methylation. However, addition of excess HCl removes the differences between the two types of ferrocene by creating a positive charge on the unmethylated nitrogen, leading to the observation of a single voltammetric wave at ~0.6 V for the oxidation of all four ferrocene residues in this compound.

Compounds **3** and **4** have four ferrocene residues in their structures, thus making them more amenable for a quantitative analysis of their voltammetric behavior than compounds **1** and **2**. Furthermore, we obtained single crystals of **3** and **4**, and the possibility of correlating solid-state structural data with voltammetric parameters collected in the solution phase increased our interest in analyzing their voltammetric behavior in a more quantitative fashion. Unfortunately, compound **3** could not be studied in much detail because of the adsorption/precipitation effects observed with its electrogenerated forms. The voltammetric behavior of compound **4** in CH_3CN was free from these adsorption effects and could be analyzed more quantitatively using digital simulations. The mechanism for the electrochemical oxidation of this compound is postulated to consist of four consecutive, one-electron transfer steps (eqs 1–4), as shown in Scheme 2. Two comproportionation equilibria must also be considered (eqs 5 and 6), with their respective equilibrium constants (K_c and K_c') given in terms of the oxidation potentials as shown in eqs 7 and 8 below.

$$\mathbf{4}^{3+} + \mathbf{4}^{+} \leftrightarrow 2\,\mathbf{4}^{2+},\ K_c \tag{5}$$

$$\mathbf{4}^{5+} + \mathbf{4}^{3+} \leftrightarrow 2\,\mathbf{4}^{4+},\ K_c' \tag{6}$$

$$K_c = \exp[({}^{2}E^{\circ\prime} - {}^{1}E^{\circ\prime})F/RT] \tag{7}$$

$$K_c' = \exp[({}^{4}E^{\circ\prime} - {}^{3}E^{\circ\prime})F/RT] \tag{8}$$

where ${}^{i}E^{\circ\prime}$ represents the formal potentials for the one-electron oxidation steps 1–4 in Scheme 2.

The electrochemical parameters (see Table 3) obtained by fitting simulated voltammograms to the experimental current–potential response of compound **4** (shown in Figure 2, continuous line) clearly indicate that the oxidation of this compound takes place in two main voltammetric waves. The first wave consists of two

---

[15] See, for instance: (a) Rulkens, R.; Lough, A. J.; Manners, I.; Lovelace, S. R.; Grant, C.; Geiger, W. E. *J. Am. Chem. Soc.* **1996**, *118*, 12683. (b) Grossmann, B.; Heinze, J.; Herdtweck, E.; Kohler, F. H.; Noth, H.; Schwenk, H.; Spiegler, M.; Wachter, W.; Weber, B. *Angew. Chem., Int. Ed. Engl.* **1997**, *36*, 387.

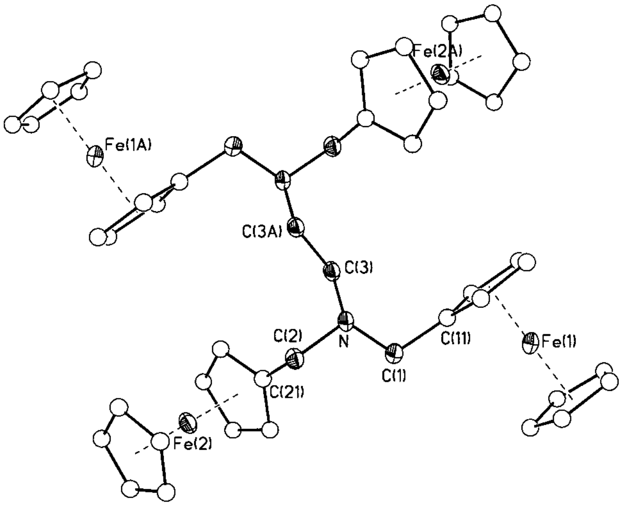

Figure 3. ORTEP plot of molecule **3** at 30% probability level.

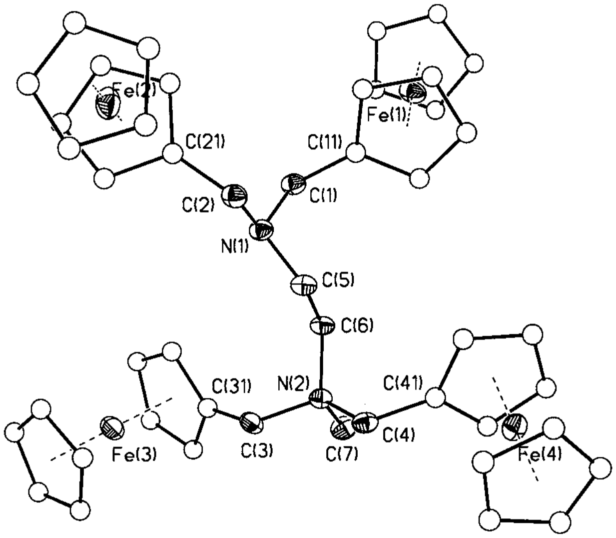

Figure 4. ORTEP plot of molecule **4** at 30% probability level.

Table 3. Electrochemical Parameters for Compound 4 (before and after protonation) Obtained from Fitting Digitally Simulated Voltammograms to the Experimental Response

parameter	unprotonated	protonated
${}^{1}E^{\circ\prime}$ (V vs Ag/AgCl)	0.426	0.586
${}^{2}E^{\circ\prime}$ (V vs Ag/AgCl)	0.504	0.611
${}^{3}E^{\circ\prime}$ (V vs Ag/AgCl)	0.626	0.608
${}^{4}E^{\circ\prime}$ (V vs Ag/AgCl)	0.697	0.676
K_c	20.8	8.2
K_c'	15.7	14.2

Table 4. Selected Bond Lengths (Å), Angles (deg), and Interatomic Distances (Å) for Compounds 3 and 4

3		4	
	Bond Lengths (Å)		
N−C(1)	1.470(3)	N(1)−C(1)	1.481(4)
N−C(2)	1.476(2)	N(1)−C(2)	1.473(4)
N−C(3)	1.464(3)	N(1)−C(5)	1.461(4)
C(3)−C(3A)	1.514(4)	N(2)−C(3)	1.532(4)
C(1)−C(11)	1.501(3)	N(2)−C(4)	1.538(4)
C(2)−C(21)	1.506(3)	N(2)−C(6)	1.515(4)
		N(2)−C(7)	1.500(4)
	Bond Angles (deg)		
C(1)−N−C(2)	112.80(17)	C(2)−N(1)−C(1)	112.4(2)
C(3)−N−C(1)	112.35(16)	C(5)−N(1)−C(1)	112.4(3)
C(3)−N−C(2)	113.36(17)	C(5)−N(1)−C(2)	109.4(3)
N−C(1)−C(11)	110.29(17)	C(6)−N(2)−C(3)	111.4(2)
N−C(2)−C(21)	116.67(17)	C(7)−N(2)−C(3)	109.3(2)
N−C(3)−C(3A)	111.8(2)	C(4)−N(2)−C(3)	106.5(2)
		C(6)−N(2)−C(4)	112.0(2)
		C(7)−N(2)−C(4)	109.0(2)
		C(7)−N(2)−C(6)	108.6(2)
	Fe−Fe Distances (Å)		
Fe1−Fe2	8.242	Fe1−Fe2	7.133
Fe1−Fe1A	11.066	Fe1−Fe3	9.436
Fe1−Fe2A	6.66	Fe1−Fe4	7.687
Fe2−Fe2A	10.105	Fe2−Fe3	9.898
		Fe2−Fe4	7.478
		Fe3−Fe4	8.647
	Shortest Edge−Edge Distance between Two Fc Units (Å)		
C11−C21	4.577	C11−C21	3.908
C14−C22A	3.798	C15−C42	3.728
		C21−C35	4.843
		C31−C41	5.048

individual one-electron steps at formal potentials of 0.426 and 0.504 V that are assigned to the oxidation of the two ferrocene residues attached to the uncharged nitrogen. The second wave is also formed by two one-electron steps, at 0.626 and 0.697 V, that are ascribed to the oxidation of the ferrocene groups attached to the quaternized, positively charged nitrogen. From these potential values, the two comproportionation constants K_c and K_c' are calculated as 21 and 16, respectively. Both values are slightly larger than the statistical limit of 4 that is predicted for two noninteracting redox centers, revealing that there is a small degree of electronic communication between each pair of ferrocene units at the two ends of the molecule.

After protonation, the voltammetric behavior of **4** changes (Figure 2, dotted line), and fitting of digitally simulated voltammograms leads to a different set of electrochemical parameters also given in Table 3. This time the four one-electron oxidation steps take place in a much narrower potential range (0.571−0.676 V), resulting in a single and rather broad voltammetric wave. A clear effect of protonation is to remove the gradient of formal potential that exists in unprotonated **4**. The calculated values of the comproportionation constants are now 8 and 14 for K_c and K_c', respectively. While the value of K_c' remains essentially constant as compared to its value before protonation, a decrease is observed in the K_c value. This is again consistent with our previous reports on the effects of protonation in dinuclear ferrocene compounds containing a $-CH_2-N(R)-CH_2-$ tether.[5]

Molecular Structures of 3 and 4. Single crystals of **3** and **4** were prepared and analyzed by X-ray diffraction methods. Structural plots of molecules **3** and **4** are shown in Figures 3 and 4, respectively, and selected bond lengths and angles are given in Table 4. The structural features of the ferrocene residues are comparable to those previously reported in the literature.[16] Notice the presence of a crystallographic inversion center in the structure of ferrocene tetramer **3** and the comparative loss of symmetry caused by the methylation of one of the nitrogen atoms in **4**. It is particularly instructive to survey the geometrical parameters around the −N− bridges in these compounds.

---

[16] Haaland, A. *Acc. Chem. Res.* **1979**, *12*, 415.

For instance, the N−C bond lengths in compound **3** and in the nonmethylated half of **4** are very similar within the experimental error margin [range 1.461(4)−1.481(4) Å]. In contrast, the N−C bond lengths in the methylated half of **4** range from 1.500(4) to 1.538(4) Å, indicating that *N*-methylation has a clear lengthening effect on these bonds. Furthermore, the through-space Fe−Fe distance between the two ferrocene centers linked to the positively charged nitrogen in **4** is 8.647 Å, which is clearly longer than the corresponding value for the remaining two ferrocene centers in the same compound (7.133 Å). The Fe−Fe distance between both pairs of ferrocene centers in compound **3** is 8.242 Å. All these solid-state data are consistent with our previously reported results[5b] on the dinuclear ferrocene building block expressed in these oligomers.

Conclusions

We have prepared and characterized four new oligomeric compounds with dendritic character containing variable numbers of ferrocene centers (4−8). Most of the ferrocene centers in these compounds are present in the form of dinuclear motifs in which two ferrocene residues are connected by a $-CH_2-N(R)-CH_2-$ tether. The electrochemical behavior of these compounds indicates that as long as the nitrogens in the connecting tethers remained uncharged, all ferrocene centers behave as essentially noninteracting, equivalent redox centers. It is however possible to differentiate some of the ferrocene centers by protonation or methylation of the corresponding nitrogen atoms, thus leading to dendritic structures having two populations of ferrocene residues with two different formal potentials.

Acknowledgment. The authors are grateful to the NSF for the generous financial support of this work (to A.E.K., CHE-9982014). T.R. acknowledges the CCD diffractometer fund from the University of Miami.

Supporting Information Available: Full tables of atomic coordinates, bond lengths and angles, and anisotropic displacements are provided (Tables S1−S8). This material is available free of charge via the Internet at http://pubs.acs.org. Full sets of crystallographic data have been deposited with the Cambridge Crystallographic Data Center (CCDC 158457 and 158458 for compounds **3** and **4**, respectively).

OM0101792